

Solvable toy model of negative energetic elasticity

Atsushi Iwaki^{1,*} and Soshun Ozaki²

¹*Department of Physics, University of Tokyo, 7-3-1 Hongo, Bunkyo-ku, Tokyo 113-0033, Japan*

²*Department of Basic Science, University of Tokyo, 3-8-1 Komaba, Meguro-ku, Tokyo 153-0041, Japan*

(Dated: September 25, 2024)

Recent experiments have established negative energetic elasticity, the negative contribution of energy to the elastic modulus, as a universal property of polymer gels. To reveal the microscopic origin of this phenomenon, Shirai and Sakumichi investigated a polymer model on a cubic lattice with the energy effect from the solvent in finite-size calculations [*Phys. Rev. Lett.* **130**, 148101 (2023)]. Motivated by this work, we provide a simple platform to study negative energetic elasticity by considering a one-dimensional random walk with the energy effect. This model can be mapped onto the classical Ising chain, leading to an exact form of the free energy in the thermodynamic or continuous limit. Our analytical results are qualitatively consistent with Shirai and Sakumichi's results. Our model serves as a fundamental benchmark for studying the elasticity of polymer chains.

Introduction. — In condensed matter physics, solvable toy models play a crucial role in understanding the essence of phenomena. For instance, entropic elasticity, which explains the elastic modulus of rubbers, appears in a one-dimensional (1D) random walk. This serves as a concrete example to comprehend how the number of possible states is converted into elasticity through statistical mechanics [1, 2].

Rubberlike materials consist of polymer chains that form entangled and crosslinked networks. The elastic modulus of these materials is determined not only by the entropic contribution but also by the energetic one. Experiments with natural and synthetic rubbers have demonstrated that the energetic contribution is negligibly small [3–5]. Consequently, the energy effect has been ignored in the well-known theories of rubber elasticity [6–9]. However, recent experiments have revealed a significant negative energetic contribution in polymer gels, which are composed of polymer networks containing a large amount of solvent [10–15]. Understanding the microscopic origins of negative energetic elasticity remains an important problem.

To address this issue, several approaches have been proposed. Shirai and Sakumichi investigated a 3D self-avoiding walk, a random walk where the overlap with itself is prohibited, by conducting an exact enumeration [16]. The self-avoiding walk is acknowledged as an effective lattice model for a single polymer chain in a dilute solution since it reproduces the excluded volume phenomena of polymers [17]. The energy effect from solvents was initially discussed in Ref. [18] and later evolved into the so-called interacting self-avoiding walk [19]. Shirai and Sakumichi treated the self-repulsive interactions of this model and derived negative energetic elasticity. In another research, Bleha and Cifra employed the Monte Carlo method to study a continuum wormlike chain [20], which represents the polymer chain as a continuous curve and the integral of the curvature gives the bending energy [21]. This model describes semiflexible polymers

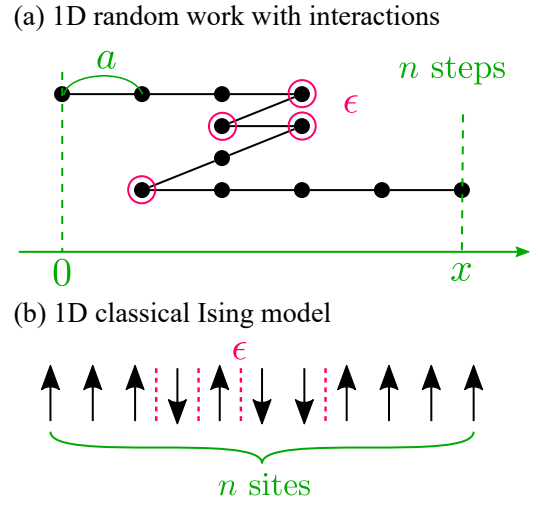


FIG. 1. Schematic illustrations for (a) a single realization of a 1D random walk with energy cost ϵ at each bending and (b) the corresponding configuration of the 1D classical Ising model.

characterized by high energy costs for bending such as a double-stranded DNA [22]. They found a negative energetic contribution to force at moderate extension, which decreases with higher extension. Additionally, Hagita *et al.* conducted all-atom molecular dynamics simulations on polyethylene glycol hydrogels [23], which was used in the first observation of negative energetic elasticity [10]. They performed these simulations under both constant-volume and constant-pressure conditions, and confirmed that the former shows stronger negativity in energetic elasticity. As a more recent work, Duarte and Rizzi proposed a simple model, a 1D random walk with independent energy at each step [24]. This model is trivially solvable because it is *non-interacting*.

There is a need for an *interacting* model that can be analytically solved in the thermodynamic limit because previous approaches rely on finite-size computations, nu-

merical simulations, or the absence of the interaction. In this Letter, we propose a simple toy model to study negative energetic elasticity by introducing an energy cost to each bend in a 1D random walk as shown in Fig. 1(a). This model can be mapped onto the 1D classical Ising model depicted in Fig. 1(b), resulting in the exact solution in the thermodynamic or continuous limit. The energy cost at each bending behaves as a self-repulsive interaction like Shirai and Sakumichi's work on the self-avoiding walk [16]. Our new model successfully explains several important features found in previous studies of negative energetic elasticity despite its simplicity. Our results are a natural extension of entropic elasticity in a 1D random walk, thus we believe that this model will be fundamental to understand the elasticity of polymer gels.

Model.— We start with a 1D random walk characterized by the number of steps n , the width per step a , and the final position x as shown in Fig. 1(a). To incorporate the energy effect, we introduce an energy term ϵ for each bending. For instance, the realization depicted in Fig. 1(a) incurs an energy cost of 4ϵ . By associating right (left) steps with up (down) spins, this model can be mapped onto the 1D classical Ising model as shown in Fig. 1(b). The Hamiltonian of this model is given by

$$\begin{aligned} H_0(\boldsymbol{\sigma}) &= \sum_{i=1}^{n-1} \epsilon \frac{1 - \sigma_i \sigma_{i+1}}{2} \\ &= -\frac{\epsilon}{2} \sum_{i=1}^{n-1} \sigma_i \sigma_{i+1} + \epsilon \frac{n-1}{2}, \end{aligned} \quad (1)$$

where $\sigma_i = \pm 1$ is the classical spin at site i , corresponding to the right/left direction of the i -th step. With an external force F_{ex} , the whole Hamiltonian becomes

$$\begin{aligned} H(\boldsymbol{\sigma}; F_{\text{ex}}) &= H_0(\boldsymbol{\sigma}) - F_{\text{ex}} a \sum_{i=1}^n \sigma_i \\ &= -\frac{\epsilon}{2} \sum_{i=1}^{n-1} \sigma_i \sigma_{i+1} - F_{\text{ex}} a \sum_{i=1}^n \sigma_i + \epsilon \frac{n-1}{2}, \end{aligned} \quad (2)$$

because the final position x is expressed by the spins as $x = a \sum_{i=1}^n \sigma_i$. These Hamiltonians are the 1D classical Ising model with and without a magnetic field up to an energy constant. Our model is a 1D version of a discrete wormlike chain [25] which is equivalent to the classical XY model.

In the following, we exactly calculate the thermodynamic functions under two independent conditions; the external force F_{ex} is fixed in the first and the final position x is fixed in the second. The first case is described by the Ising model in a magnetic field, whereas the second case is described by the Ising model with a fixed magnetization. The force-fixed and position-fixed conditions correspond to the constant-pressure and constant-volume condition of all-atom molecular dynamics in Ref. [23], re-

spectively. Under both conditions, we can obtain the relationship between x and F_{ex} by differentiating the thermodynamic functions. This relationship allows us to calculate the stiffness $k = \partial F_{\text{ex}} / \partial x$, which represents the elastic modulus of a single chain, including its energetic and entropic contributions.

Force-fixed condition.— The force-fixed condition is represented by the Hamiltonian in Eq. (2). Consequently, the partition function at the temperature $k_B T = 1/\beta$ is given by

$$Z_g(\beta, F_{\text{ex}}, n) = \sum_{\boldsymbol{\sigma}} e^{-\beta H(\boldsymbol{\sigma}; F_{\text{ex}})}. \quad (3)$$

The free energy associated with this partition function can be calculated using the traditional transfer-matrix method [26]. The partition function is represented by the transfer matrix as

$$Z_g(\beta, F_{\text{ex}}, n) = \mathbf{v}^\top X^{n-1} \mathbf{v}, \quad (4)$$

where

$$X = \begin{bmatrix} e^{\beta F_{\text{ex}} a} & e^{-\beta \epsilon} \\ e^{-\beta \epsilon} & e^{-\beta F_{\text{ex}} a} \end{bmatrix}, \quad \mathbf{v} = \begin{bmatrix} e^{\beta F_{\text{ex}} a / 2} \\ e^{-\beta F_{\text{ex}} a / 2} \end{bmatrix}. \quad (5)$$

From the largest eigenvalue of X , the Gibbs free energy, the thermodynamic function under this condition, can be calculated as

$$\begin{aligned} \beta g_{\text{th}}(\beta, F_{\text{ex}}) &= -\lim_{n \rightarrow \infty} \frac{1}{n} \log Z_g(\beta, F_{\text{ex}}, n) \\ &= -\log \left[\cosh(\beta F_{\text{ex}} a) + \sqrt{\sinh^2(\beta F_{\text{ex}} a) + e^{-2\beta \epsilon}} \right]. \end{aligned} \quad (6)$$

The relationships between F_{ex} and x is determined through $x/n = -\partial g_{\text{th}} / \partial F_{\text{ex}}$ as

$$\sinh(\beta F_{\text{ex}} a) = e^{-\beta \epsilon} \frac{y}{\sqrt{1 - y^2}}, \quad (7)$$

where $y = x/na$ is the rescaled dimensionless position. The stiffness $k = \partial F_{\text{ex}} / \partial x$ can be calculated as a function of β and y :

$$\hat{\beta} \hat{k}(\hat{\beta}, y) = \frac{e^{-\hat{\beta}}}{1 - y^2} \sqrt{\frac{1}{1 + (e^{-2\hat{\beta}} - 1)y^2}}. \quad (8)$$

Here, we have introduced rescaled dimensionless quantities $\hat{k} = na^2 k / \epsilon$ and $\hat{\beta} = \beta \epsilon$.

In order to decompose the stiffness into its energetic and entropic contributions as $k = k_U + k_S$ [10], we consider the Helmholtz free energy $f_{\text{th}}(\beta, x)$, which is the thermodynamic function under the position-fixed condition calculated in the next part explicitly. Since we can obtain F_{ex} by the differentiation of f_{th} as $F_{\text{ex}}/n = \partial f_{\text{th}} / \partial x$, the stiffness is given by $k/n = \partial^2 f_{\text{th}} / \partial x^2$. Considering that f_{th} is decomposed into the energetic and

entropic term as $f_{\text{th}} = u - Ts$, the energetic and entropic contributions to the stiffness can be defined as $k_U/n = \partial^2 u/\partial x^2$ and $k_S/n = -T \partial^2 s/\partial x^2$, respectively. By applying Maxwell's relation, both contributions can be computed from $k(T, x)$ as $k_S = T \partial k/\partial T$ and $k_U = k - k_S$.

By substituting the equilibrium value $y = 0$ when $F_{\text{ex}} = 0$, the stiffness and its energetic and entropic contributions are derived from Eq. (8) as

$$\hat{\beta} \hat{k} = e^{-\hat{\beta}}, \quad \hat{\beta} \hat{k}_U = -\hat{\beta} e^{-\hat{\beta}}, \quad \hat{\beta} \hat{k}_S = (1 + \hat{\beta}) e^{-\hat{\beta}}, \quad (9)$$

where $\hat{k}_U = na^2 k_U/\epsilon$ and $\hat{k}_S = na^2 k_S/\epsilon$ are rescaled dimensionless quantities. Therefore, when the interactions are repulsive ($\epsilon > 0$), the energetic contribution becomes negative ($k_U < 0$), indicating negative energetic elasticity. As will be plotted later, the behavior of Eq. (9) is qualitatively consistent with Fig. 3 of Ref. [16] on the interacting self-avoiding walk.

In the vicinity of a temperature T_0 , the stiffness is approximated by

$$k(T) \simeq \frac{k_S(T_0)}{T_0} T + k_U(T_0). \quad (10)$$

Therefore, in experiments and numerical simulations, when the stiffness is linearly approximated as $k(T) \simeq a(T - T_U)$, a dimensionless quantity

$$\hat{T}_U = \frac{k_B T_U}{\epsilon} = -\frac{k_U(T_0) k_B T_0}{k_S(T_0) \epsilon} \quad (11)$$

is used as an indicator of negative energetic elasticity. We can analytically obtain \hat{T}_U in the limit of $T_0 \rightarrow \infty$ as

$$\hat{T}_U^\infty = \lim_{T_0 \rightarrow \infty} \hat{T}_U(T_0) = 1 - y^2, \quad (12)$$

indicating that negative energy elasticity diminishes as the chain is extended. This result is consistent with the previous work on the wormlike chain [20].

Although the equilibrium value is $y = 0$ when $F_{\text{ex}} = 0$, the chain is considered to be extended by thermal fluctuations. Here, we investigate the mean square of the position $\langle y^2 \rangle$. Using the Gibbs free energy in the thermodynamic limit, the mean square is calculated as

$$\langle y^2 \rangle = -\frac{1}{n} \frac{\partial^2 g_{\text{th}}}{\partial F_{\text{ex}}^2}(\beta, F_{\text{ex}} = 0) = \frac{e^{\beta\epsilon}}{n}. \quad (13)$$

Thus, $y = 0$ is the stable equilibrium value in the thermodynamic limit $n \rightarrow \infty$. Since $\langle y^2 \rangle$ is bounded by 1, this equality approximately holds if $e^{\beta\epsilon} \ll n$. In contrast, if $e^{\beta\epsilon} \gg n$, the mean square saturates to $\langle y^2 \rangle \simeq 1$. To explore the temperature region where $e^{\beta\epsilon}$ and n are comparable, we perform a finite-size scaling analysis [27]. By fixing $\alpha = n/e^{\beta\epsilon}$ and taking the limit $n \rightarrow \infty$, we obtain

$$\langle y^2 \rangle = \frac{e^{-2\alpha} - 1 + 2\alpha}{2\alpha^2}. \quad (14)$$

This form of scaling function explains the behavior mentioned above. By taking the same scaling limit, we can represent the stiffness as a function of α as

$$\hat{\beta} \tilde{k} = \frac{1}{\langle y^2 \rangle} = \frac{2\alpha^2}{e^{-2\alpha} - 1 + 2\alpha}, \quad (15)$$

where $\tilde{k} = n^2 a^2 k/\epsilon$ is a rescaled quantity for this limit. The energetic component of the stiffness also conforms to a scaling function as

$$\tilde{k}_U = \frac{\partial}{\partial \hat{\beta}} \hat{\beta} \tilde{k} = -4\alpha^2 \frac{(1 + \alpha)e^{-2\alpha} - 1 + \alpha}{(e^{-2\alpha} - 1 + 2\alpha)^2}, \quad (16)$$

where $\tilde{k}_U = n^2 a^2 k_U/\epsilon$ is a rescaled quantity. In the regime where $\alpha \ll 1$, indicating the chain is fully extended due to thermal fluctuations, the stiffness is polynomially suppressed with inverse temperature as $\tilde{k} \simeq 1/\beta\epsilon$. On the other hand, its energetic contribution is exponentially small, expressed as $\tilde{k}_U \simeq -2n/3e^{\beta\epsilon}$. Consequently, the ratio of the energetic part to the stiffness decreases with a chain extension, aligning with Eq. (12).

Position-fixed condition.— The position-fixed condition corresponds to the Ising model with a fixed magnetization, where the partition function is given by

$$Z_f(\beta, x, n) = \sum_{\sigma} e^{-\beta H_0(\sigma)} \delta\left(\frac{x}{a}, \sum_{i=1}^N \sigma_i\right). \quad (17)$$

We categorize the summation based on the number of bends as

$$Z_f(\beta, x, n) = \sum_m W(m, x, n) e^{-\beta\epsilon m}, \quad (18)$$

where $W(m, x, n)$ is the number of cases of m -bending realizations with the final position x of a n -step random walk. Since $W(m, x, n)$ does not depend on the sign of x , we have $Z_f(\beta, x, n) = Z_f(\beta, -x, n)$. Denoting the number of right and left steps as

$$n_R = \frac{n}{2} + \frac{x}{2a}, \quad n_L = \frac{n}{2} - \frac{x}{2a}, \quad (19)$$

and assuming $x \geq 0$, i.e., $n_R \geq n_L$, $W(m, x, n)$ is evaluated by division into four cases: the random walks starting with the right/left step and ending with the right/left step. Therefore, we obtain the partition function as

$$\begin{aligned} Z_f(\beta, x, n) = & 2 \sum_{m=1}^{n_L} \binom{n_R - 1}{m - 1} \binom{n_L - 1}{m - 1} e^{-(2m-1)\beta\epsilon} \\ & + \sum_{m=1}^{n_L} \binom{n_R - 1}{m} \binom{n_L - 1}{m - 1} e^{-2m\beta\epsilon} \\ & + \sum_{m=1}^{n_L - 1} \binom{n_R - 1}{m - 1} \binom{n_L - 1}{m} e^{-2m\beta\epsilon}. \end{aligned} \quad (20)$$

The logarithm of this summation can traditionally be evaluated using the maximum-term method in the thermodynamic limit [28]. Instead, we will evaluate the summation by inserting the Kronecker delta and obtain an exact integral form of the partition function. This approach enables us not only to calculate the free energy in the thermodynamic limit but also to account for finite-size correction terms in the numerical part and perform the finite-size scaling similar to the previous section. First, we insert a Kronecker delta in an integral form,

$$\delta_{lm} = \frac{1}{2\pi i} \oint_C \frac{dz}{z} z^{l-m}, \quad (21)$$

where C is a counterclockwise contour around the origin.

By carrying out the summation, we obtain the partition function in an integral form as

$$Z_f(\beta, x, n) = \frac{e^{-\beta\epsilon}}{\pi i} \oint_C \frac{dz}{z} (1 + e^{-\beta\epsilon} z)^{n_{\text{R}}-1} \times (1 + e^{-\beta\epsilon} z^{-1})^{n_{\text{L}}-1} \left(1 + \frac{z + z^{-1}}{2}\right). \quad (22)$$

This representation also holds when $x < 0$ because the change of the variable $z \rightarrow w = 1/z$ confirms $Z_f(\beta, x, n) = Z_f(\beta, -x, n)$. Applying the saddlepoint approximation, we obtain the Helmholtz free energy, the thermodynamic function under this condition, as

$$\beta f_{\text{th}}(\beta, y) = - \lim_{n \rightarrow \infty} \frac{1}{n} \log Z_f(\beta, nay, n) = - \frac{1+y}{2} \log \left[1 + (1 - e^{-2\beta\epsilon})y + e^{-\beta\epsilon} \sqrt{1 - (1 - e^{-2\beta\epsilon})y^2} \right] - \frac{1-y}{2} \log \left[1 - (1 - e^{-2\beta\epsilon})y + e^{-\beta\epsilon} \sqrt{1 - (1 - e^{-2\beta\epsilon})y^2} \right] + \frac{1+y}{2} \log(1+y) + \frac{1-y}{2} \log(1-y). \quad (23)$$

This expression and the relation $F_{\text{ex}}a = \partial f_{\text{th}}/\partial y$ also leads to Eq. (7). This is because the Helmholtz free energy $f_{\text{th}}(\beta, y)$ contains the same information as the Gibbs free energy $g_{\text{th}}(\beta, F_{\text{ex}})$. These two thermodynamic functions are connected to each other through the Legendre transformation as

$$g_{\text{th}}(\beta, F_{\text{ex}}) = \min_y [f_{\text{th}}(\beta, y) - F_{\text{ex}}ay], \quad (24)$$

$$f_{\text{th}}(\beta, y) = \max_{F_{\text{ex}}} [g_{\text{th}}(\beta, F_{\text{ex}}) + F_{\text{ex}}ay]. \quad (25)$$

Numerical demonstrations.— Here, we examine our analytical results and compare them to finite-size numerical results with $n = 20$ under the force-fixed and position-fixed conditions. In addition, we demonstrate the finite-size scaling with $F_{\text{ex}} = 0$ for various system sizes.

Figures 2(a) and (b) show the thermodynamic functions under both conditions in Eqs. (6) and (23). Under the force-fixed condition, the equilibrium value of F_{ex} is determined by maximizing $g_{\text{th}} + F_{\text{ex}}ay$ following Eq. (25). Thus, the Gibbs free energy βg_{th} is convex upward as seen in Fig. 2(a). On the other hand, the equilibrium value of y is obtained by minimizing $f_{\text{th}} - F_{\text{ex}}ay$ following Eq. (24) under the position-fixed condition, resulting in a convex downward behavior of the Helmholtz free energy βf_{th} as illustrated in Fig. 2(b). The data points in Fig. 2(a) are consistent with the analytical results. However, in Fig 2(b), the raw numerical data represented by circle points differs from the exact solutions due to the finite-size effect. Detailed calculation of the saddle point

approximation in Eq. (23) allows us to evaluate the dominant term of this finite-size effect as

$$-\frac{1}{n} \log Z_f(\beta, nay, n) \simeq \beta f_{\text{th}}(\beta, y) + \frac{1}{2n} \log n. \quad (26)$$

This dominant term $\log n/2n$, which is independent of β and y , does not affect energy, external force, and stiffness. We modify the numerical results by subtracting the dominant term $\log n/2n$ from the finite-size calculations of the free energy. The modified numerical results shown in Fig. 2(b) with square dots are in improved agreement with the exact solutions.

We decompose the Helmholtz free energy βf_{th} into the energy βu and entropy s/k_B , which are shown in Figs. 2(c) and (d), respectively. Because the energetic and entropic contributions to the stiffness are determined by the second derivative of these quantities, the convexity observed in Figs. 2(c) and (d) characterizes each contribution to elasticity. When the interaction is repulsive as $\epsilon > 0$, βu displays upward convexity, indicating negative energetic elasticity. In the self-attractive case with $\epsilon < 0$, the entropy becomes convex downward near $y = 0$ at low temperature, which means negative entropic elasticity. After removing the finite-size effect according to Eq. (26), the numerical results are in good agreement with the exact solutions.

The relation between the external force $\beta F_{\text{ex}}a$ and final position y in Eq. (7) is plotted in Fig. 3. The numerical data are generated by differentiating the thermodynamic functions shown in Figs. 2(a) and (b). For the position-fixed condition, $\beta F_{\text{ex}}a$ is approximated using a

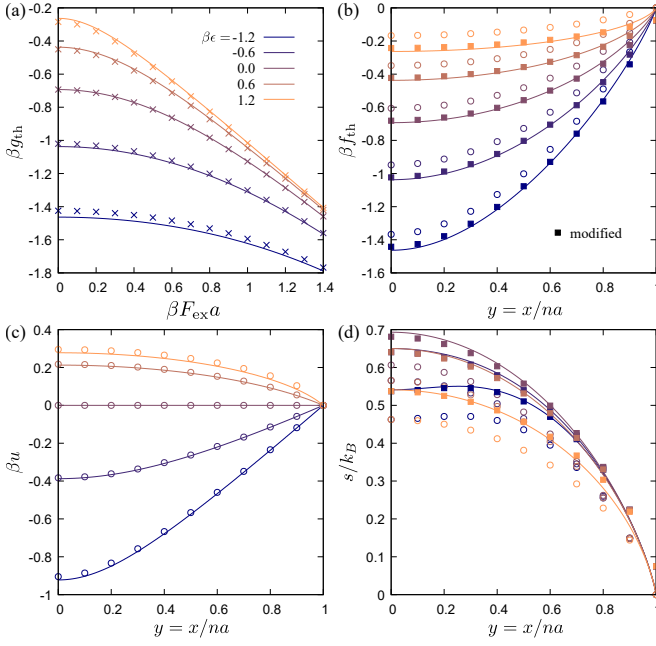


FIG. 2. (a) Gibbs free energy βg_{th} under the force-fixed condition in Eq. (6) and (b) Helmholtz free energy βf_{th} under the position-fixed condition in Eq. (23). (c) Energy βu and (d) entropy s/k_B as functions of $y = x/na$ obtained from the Helmholtz free energy βf_{th} . These quantities are computed for $\beta\epsilon = 0, \pm 0.6, \pm 1.2$. Data points represent numerical results with $n = 20$. Square points in panels (b) and (d) express modified results to remove the dominant term of the finite-size effect in Eq. (26).

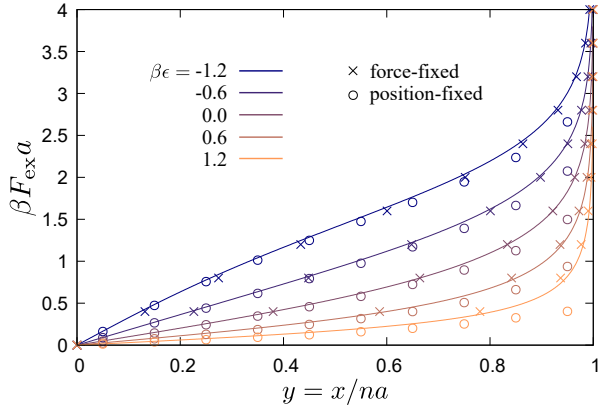


FIG. 3. Relationship between the external force $\beta F_{\text{ex}} a$ and the final position $y = x/na$ in Eq. (7) for various $\beta\epsilon$. Cross (\times) and circle (\circ) points represent numerical results with $n = 20$ under the force-fixed and position-fixed conditions, respectively.

finite difference form as

$$\beta F_{\text{ex}} a \left(y + \frac{\Delta y}{2} \right) \simeq \frac{\beta f_{\text{th}}(y + \Delta y) - \beta f_{\text{th}}(y)}{\Delta y}, \quad (27)$$

where $\Delta y = 2/na$. As expected, the stronger force is required to extend the chain for the larger $\beta\epsilon$. The

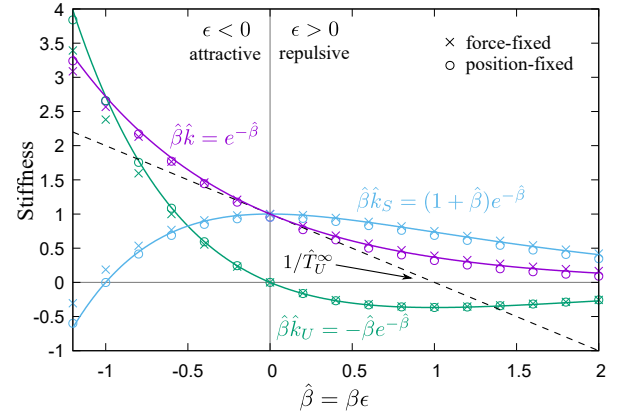


FIG. 4. Stiffness $\hat{\beta} \hat{k}$ and its energetic and entropic contributions, $\hat{\beta} \hat{k}_U$ and $\hat{\beta} \hat{k}_S$, with the final position $y = 0$ in Eq. (9). Cross (\times) and circle (\circ) points represent numerical results with $n = 20$ under the force-fixed condition at $F_{\text{ex}} = 0$ and the position-fixed condition at $y = 0$, respectively. The tangent line of $\hat{\beta} \hat{k}$ at $\hat{\beta} = 0$ depicted by a dashed line intersects the horizontal axis at $1/\hat{T}_U^\infty$.

numerical results under the force-fixed condition show good agreement with the exact solutions across the whole range, while discrepancies arise at high extensions under the position-fixed condition. This is because the finite-size effect depends on the ensemble used; it is exponentially small in the force-fixed condition and polynomially small in the position-fixed condition.

Figure 4 displays the stiffness and its energetic and entropic contributions at $y = 0$ in Eq. (9). The numerical data are derived from the second derivative of the thermodynamic functions shown in Figs. 2(a) and (b) at $F_{\text{ex}} = 0$ or $y = 0$, employing a finite-difference form for the position-fixed case as

$$\hat{\beta} \hat{k}(y) \simeq \frac{\beta f_{\text{th}}(y + \Delta y) - 2\beta f_{\text{th}}(y) + \beta f_{\text{th}}(y - \Delta y)}{(\Delta y)^2}. \quad (28)$$

We observe negative energetic elasticity in the self-repulsive region with $\epsilon > 0$ and negative entropic elasticity in the self-attractive ($\epsilon < 0$) and low-temperature region, which aligns with the convexity seen in Figs. 2(c) and (d). The dashed line represents the tangent line of $\hat{\beta} \hat{k}$ at $\hat{\beta} = 0$. This line crosses the horizontal axis at $1/\hat{T}_U^\infty$, which is determined analytically in Eq. (12); in this case with $y = 0$, $\hat{T}_U^\infty = 1$. The numerical results are almost coincident with the exact solutions for both conditions. The qualitative behavior of Fig. 4 is consistent with those reported in Fig. 3 of Ref. [16] on the interacting self-avoiding walk.

Figure 5 shows the finite-size scaling analysis for the mean square position, the stiffness, and its energetic contribution under the condition $F_{\text{ex}} = 0$. The numerical result for $n = 10$ already closely align with the scaling functions described in Eqs. (14), (15), and (16) across

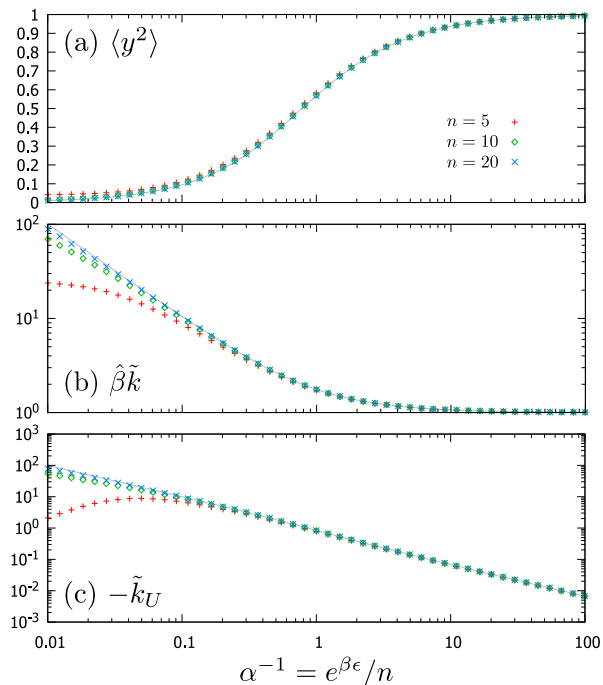


FIG. 5. (a) The means square of the position $\langle y^2 \rangle$, (b) the stiffness $\hat{\beta}\tilde{k}$, and (c) its energetic contribution $-\tilde{k}_U$ as functions of $\alpha^{-1} = e^{\beta\epsilon}/n$ for $n = 5, 10, 20$ when $F_{\text{ex}} = 0$. Solid lines represent the scaling functions in Eqs. (14), (15), and (16).

a broad temperature range. As illustrated in Fig. 5(b), $\hat{\beta}\tilde{k}$ becomes constant at high temperature $e^{\beta\epsilon} \gg n$. In contrast, Fig. 5(c) demonstrates that \tilde{k}_U continues to decrease over the whole temperature range. Consequently, the negative energetic elasticity reduces as the chain elongates due to thermal fluctuations.

Summary and discussion.— We have proposed a toy model to explore negative energetic elasticity, a 1D random walk with an energy cost ϵ for each bending. This model can be mapped onto the 1D classical Ising model by associating right (left) steps with up (down) spins. Table I shows how these models correspond. We have exactly calculated the thermodynamic functions under the force-fixed and position-fixed conditions in Eqs. (6) and (23) using the transfer-matrix formulation and saddle-point approximation. The Legendre transformation connects these thermodynamic functions as they are equivalent. We analytically obtained the stiffness in Eq. (8), which has a negative energetic contribution when the interaction is repulsive as $\epsilon > 0$.

Our model reproduces several properties of previous studies on negative energetic elasticity. The stiffness and its energetic and entropic contributions in the simplest case in Eq. (9) plotted in Fig. 4 are qualitatively consistent with the results of a 3D self-avoiding walk in Fig. 3 of Ref. [16]. Equation (12) shows that the negative energetic contribution decreases compared to the

TABLE I. Correspondence between the 1D random walk with interactions and the 1D classical Ising model.

Random walk	Ising model
right/left step	up/down spin
external force F_{ex}	magnetic field h
final position x	magnetization M
stiffness $k = \frac{\partial F_{\text{ex}}}{\partial x}$	(susceptibility) $^{-1}$ $\chi^{-1} = \left(\frac{\partial M}{\partial h}\right)^{-1}$

entropic one with chain extension, in accordance with Ref. [20] for a continuum wormlike chain. The force-fixed (position-fixed) condition of our model corresponds to the constant-pressure (constant-volume) condition of all-atom molecular dynamics simulations in Ref. [23]. Therefore, the finite-size effect in these simulations may resemble our model. In this sense, our model serves as an essential platform for investigating the elasticity of polymer chains.

In addition to reproducing existing findings, we have succeeded in characterizing the behavior of stiffness in the regime where thermal fluctuations extend the chain as scaling functions in Eqs. (15) and (16), plotted in Fig. 5. Our work provides a guideline for understanding the stiffness behavior resulting from changes in the folding structure of polymers which is more effective in higher-dimensional spaces.

We can extend our model to d -dimensional space with $d > 1$. In this space, steps in each direction are mapped onto one of $2d$ possible states arranged in a line and the energy cost for bending becomes interactions between different states adjacent to each other. This framework leads to the $2d$ -state Potts model in 1D, which can also be analytically solved under the fixed-force condition using the transfer-matrix method.

Acknowledgments.— We thank Yuta Sakai for comments on the Ising model. We are also grateful to Naoyuki Sakumichi and Hidehiro Saito for fruitful discussions. A. I. and S. O. were supported by a Grant-in-Aid for JSPS Research Fellow (Grants No. 22KJ0661 and No. 22KJ0988).

* atsushi-iwaki@phys.s.u-tokyo.ac.jp

- [1] C. Kittel, *Thermal Physics* (Wiley, New York, 1969).
- [2] R. Kubo, *Statistical Mechanics: An Advanced Course with Problems and Solutions* (North-Holland Physics, New York, 1988).
- [3] K. H. Meyer and C. Ferri, Sur l'élasticité du caoutchouc, *Helvetica Chimica Acta* **18**, 570–589 (1935).
- [4] R. L. Anthony, R. H. Caston, and E. Guth, Equations of state for natural and synthetic rubber-like materials. I. unaccelerated natural soft rubber, *The Journal of Physical Chemistry* **46**, 826–840 (1942).

- [5] J. E. Mark, Thermoelastic results on rubberlike networks and their bearing on the foundations of elasticity theory, *Journal of Polymer Science: Macromolecular Reviews* **11**, 135–159 (1976).
- [6] P. J. Flory, *Principles of Polymer Chemistry* (Cornell University Press, Ithaca, 1953).
- [7] H. M. James and E. Guth, Statistical thermodynamics of rubber elasticity, *The Journal of Chemical Physics* **21**, 1039–1049 (1953).
- [8] P. J. Flory, *Statistical Mechanics of Chain Molecules* (Wiley Interscience, New York, 1969).
- [9] P. J. Flory, Theory of elasticity of polymer networks. the effect of local constraints on junctions, *The Journal of Chemical Physics* **66**, 5720–5729 (1977).
- [10] Y. Yoshikawa, N. Sakumichi, U.-i. Chung, and T. Sakai, Negative energy elasticity in a rubberlike gel, *Phys. Rev. X* **11**, 011045 (2021).
- [11] N. Sakumichi, Y. Yoshikawa, and T. Sakai, Linear elasticity of polymer gels in terms of negative energy elasticity, *Polymer Journal* **53**, 1293–1303 (2021).
- [12] T. Fujiyabu, T. Sakai, R. Kudo, Y. Yoshikawa, T. Katashima, U.-i. Chung, and N. Sakumichi, Temperature dependence of polymer network diffusion, *Phys. Rev. Lett.* **127**, 237801 (2021).
- [13] T. Aoyama and K. Urayama, Negative and positive energetic elasticity of polydimethylsiloxane gels, *ACS Macro Letters* **12**, 356–361 (2023).
- [14] J. Tang, R. H. Colby, and Q. Chen, Revisiting the elasticity of tetra-poly(ethylene glycol) hydrogels, *Macromolecules* **56**, 2939–2946 (2023).
- [15] J. Tang, X. Duan, and Q. Chen, Temperature dependence of the gel modulus depends on change of solvent quality, *Macromolecules* **56**, 8574–8580 (2023).
- [16] N. C. Shirai and N. Sakumichi, Solvent-induced negative energetic elasticity in a lattice polymer chain, *Phys. Rev. Lett.* **130**, 148101 (2023).
- [17] N. Madras and G. Slade, *The Self-Avoiding Walk* (Birkhäuser Boston, 1996).
- [18] W. J. C. Orr, Statistical treatment of polymer solutions at infinite dilution, *Transactions of the Faraday Society* **43**, 12 (1947).
- [19] C. Vanderzande, *Lattice Models of Polymers* (Cambridge University Press, 1998).
- [20] T. Bleha and P. Cifra, Energy/entropy partition of force at DNA stretching, *Biopolymers* **113** (2022).
- [21] O. Kratky and G. Porod, Röntgenuntersuchung gelöster fadenmoleküle, *Recueil des Travaux Chimiques des Pays-Bas* **68**, 1106–1122 (1949).
- [22] C. P. Broedersz and F. C. MacKintosh, Modeling semiflexible polymer networks, *Rev. Mod. Phys.* **86**, 995 (2014).
- [23] K. Hagita, S. Nagahara, T. Murashima, T. Sakai, and N. Sakumichi, All-atom molecular dynamics simulations of poly(ethylene glycol) networks in water for evaluating negative energetic elasticity, *Macromolecules* **56**, 8095–8105 (2023).
- [24] L. K. R. Duarte and L. G. Rizzi, On the origin of the negative energy-related contribution to the elastic modulus of rubber-like gels, *The European Physical Journal E* **46** (2023).
- [25] A. Rosa, T. X. Hoang, D. Marenduzzo, and A. Maritan, Elasticity of semiflexible polymers with and without self-interactions, *Macromolecules* **36**, 10095–10102 (2003).
- [26] R. J. Baxter, *Exactly Solved Models in Statistical Mechanics* (Academic Press, London, 1982).
- [27] T. Antal, M. Droz, and Z. Rácz, Probability distribution of magnetization in the one-dimensional ising model: effects of boundary conditions, *Journal of Physics A: Mathematical and General* **37**, 1465–1478 (2004).
- [28] T. L. Hill, *An Introduction to Statistical Thermodynamics* (Addison-Wesley Publishing, Reading MA, 1960).